Send Orders for Reprints to reprints@benthamscience.ae

Current Organic Synthesis, **2017**, *14*, 1-11

RESEARCH ARTICLE

Design, Synthesis and Docking study of Novel Imidazolyl Pyrazolopyridine Derivatives as Antitumor Agents Targeting MCF7 Cell Line

Mohamed A. El-Borai, Mohamed K. Awad, H.F. Rizk and Faten M. Atlam*

Department of Chemistry, Faculty of Science, Tanta University, Tanta 31527, Egypt

ARTICLE HISTORY

Received: November 13, 2016
Revised: February 14, 2017
Accepted: April 25, 2017

DOI:
10.2174/1570179414666170512125759

Abstract: The cyanoacetylationof1-methyl imidazole moiety gave 3-oxoproponanitrile **I**, which upon cyclization gave the corresponding 5-amino pyrazole **II**. The reaction of compound **II** with some reactive methylene reagents gave the corresponding imidazolyl pyrazolopyridine derivatives **IIIa-e**. The synthesized compounds were prepared by conventional heating and microwave irradiation technique. The structure of the prepared compounds was confirmed by different spectroscopic tools. The compounds **IIIa-e** were tested for antitumor activity against breast cancer cell line. The quantum chemical, molecular docking and SAR studies were performed for the prepared compounds. The quantum chemical descriptors confirmed that inhibitor1-(4-methoxyphenyl)-3-(1-methyl-1*H*-imidazol-4-yl)-6-phenyl-1*H*-pyrazolo[3,4-b]- pyridine-4-ol (**IIIb**) is the most potent and reactive one among the investigated compounds. This conclusion is congruent with the results obtained experimentally.

Keyword: 5-aminopyrazole, imidazolyl pyrazolopyridine, antitumor, DFT study, molecular docking, SAR.

1. INTRODUCTION

Many functionalized imidazoles behave as antibiotics [1], fungicides [2], antiulceretics [3], antidiabetics, antihypertensive and anti-inflammatory agents [4]. The 3-oxopropano- nitriles represent a category of versatile synthetic intermediate for the synthesis of pyrazole moiety [5, 6].

Pyrazolo [3,4-*b*] pyridine skeleton is an interesting class of heterocycles due to its diverse biological properties including antitumor, antioxidant and antibacterial activities [7-18].

This attempt was made to provide a synergistic cytotoxic activity from the combination of pyrazole and imidazole moieties, resulting novel analogues, and evaluate their antitumor activity.

The addition of computer-aided drug design (CADD) technologies to the research and drug discovery approaches could lead to a reduction of up to 50% in the cost of drug design. Designing a drug is the process of finding or creating a molecule which has a specific activity on a biological organism. Development and drug discovery is a time-consuming, expensive, and interdisciplinary process whereas scientific advancements during the past two decades have altered the way of pharmaceutical research producing new bioactive molecules.

Development of powerful computer software and hardware will enable extensive studies of the protein structure and dynamics of new potential drug targets, a new challenge in the validation and calibration of computerized methods of bio-simulation. Quantum mechanical (QM) methods became popular in computational drug design and development mainly because the high accuracy is often required to estimate (relative) binding affinity allowing one to compute the binding interaction at the atomic level. However, as the macromolecules involved (in general, proteins) are very large, it is necessary to achieve a compromise between the computational cost of the calculations and the accuracy required to obtain trustful results [19, 20].

*Address correspondence to this author at the Department of Chemistry, Faculty of Science, Tanta University, Tanta 31527, Egypt; Tel: 00201200384830; Fax: 002-040-3350804; E-mail: faten.atlam@science.tanta.edu.eg

2. RESULTS AND DISCUSSION

2.1. Chemistry

Scheme (**1**) explains the reaction pathway for compounds **I**, **II** and **IIIa-e** derivatives. Compound **I** was synthesized by cyanoacetylation of 1-methyl imidazole by using cyanoacetic acid and acetic anhydride at 60-70 ^{o}C. The cyclization of corresponding β-ketonitrile [3-(1-methyl-1*H*-imidazol-4-yl)-3-oxopropanenitrile] **I** with *p*-anisyl hydrazine hydrochloride in absolute ethanol for 4 h gave the corresponding 5-amino pyrazole **II**.

Condensation of 1-(4-methoxyphenyl)-3-(1-methyl-1*H*-imidazol-4-yl)-1*H*-pyrazol-5-amine **lI** with some active methylene compounds in acetic acid as ethyl acetoacetate, ethyl benzoylacetate, ethyl cyanoacetate, diethyl malonate and acetyl acetone in acetic acid for 5-8 h gave3-imidazolyl pyrazolo[3,4-b]pyridines **IIIa-e**. The synthesized compounds were confirmed by IR, ^{1}HNMR, ^{13}CNMR and mass spectra (see experimental part).

The microwave irradiation as a source of energy was used to improve the yield and to reduce the time of the reaction. Under this technique, interesting results were obtained, and the reaction time was reduced from 4-8 hours to 15-25 min. The yield of the reactions for conventional heating was from 65% to 76 %, while for microwave irradiation, it was from 81% to 92%. Also, the obtained products were cleaner. The obtained data for the synthesized compounds were mentioned in experimental part.

1570-1794/17 $58.00+.00

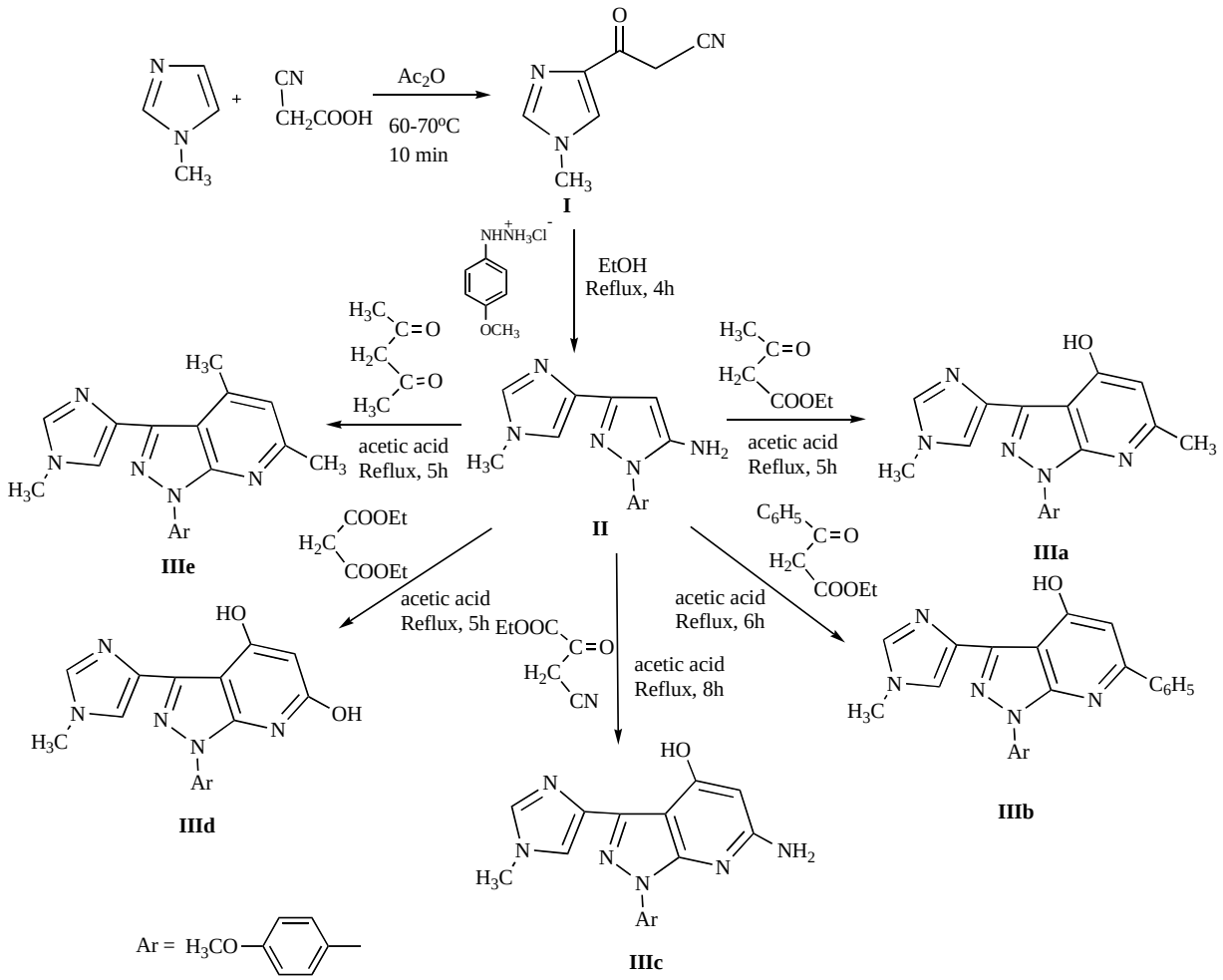

Scheme 1. Synthesis of 3-(1-methyl-1H-imidazol-4-yl)-3-oxopropanenitrile **(I)**, 1-(4-methoxyphenyl)-3-(1-methyl-1H-imidazol-4-yl)-1H-pyrazol-5-amine **(II)**, and imidazolyl-pyrazolo[2,3-b]pyridines (**IIIa-e**).

2.2. Pharmacology

2.2.1. Antitumor Evaluation

The search for novel drugs is still a priority goal for cancer therapy due to the rapid development of resistance to multiple chemotherapeutic drugs. In addition, the high toxicity is usually associated with the cancer chemotherapy drugs and their undesirable side effects increase the demand for novel antitumor active drugs against untreatable tumors with fewer side effects and/or with greater therapeutic efficiency [21]. Breast cancer is a major health problem worldwide [22]. Breast cancer is the most frequently diagnosed cancer and causes death in females worldwide, accounting for 23% (1.38 million) of the total new cancer cases and 14% (458,400) of the total cancer death in 2008 [23].

2.2.2. Antitumor Activity

The anticancer activities of compounds **IIIa-e** were investigated on one human cancer MCF7 (breast cancer) in the National Cancer Institute, Cairo University. The screening involved the calculation of the percentage growth of surviving fraction of the compound-treated cell lines compared with the untreated control using Sulforhodamie B (SRB)colorimetric assay. Sulforhodamie B is a bright pink aminoxanthene anionic dye with two sulfonic acid groups that bind electrostatically to the protein basic amino acid residues of trichloroacetic acid fixed cells under mild acidic conditions. Cultures fixed with trichloroacetic acid were stained for 30 min with 0.4% w/v Sulforhodamie B dissolved in 1% acetic acid, and the protein bound dye was extracted with 10 mM trisbase for the determination of optical density in a computer-interfaced, 96-well microtiter plate reader Skehan *et al.* [24]. The measured optical density is linear to the cell number of the surviving fraction. Therefore, the assay is a sensitive measurement of compound-induced cytotoxicity with the best signal to noise ratio. The assay also provides a colorimetric end point that is nondestructive, indefinitely stable and visible to naked eye. Data were collected, revised and analyzed by SPSS statistical package version 11. Excel computer program was used to tabulate the results (Table **1**). Probit regression analysis procedure are introduced to select the best model that describes the relationship between the probit (percentages of protection) as a dependent variable in order to be used for the prediction of the concentration of the compound that caused inhibition of 50% (IC_{50}) of cancer cells. In vitro, the growth inhibition properties of each compound were described by IC_{50} and the degree of inhibition of cancer cell line was calculated by the equation:

The probit (P) = intercept + (regression coefficient x Conc.)

Antitumor activities of the tested compounds were measured using SRB assay for the breast cancer (Fig. **1**). The overall results indicated that the tested compounds **IIIa-e** have antitumor activity with IC_{50} ranged from 16.6-19.3µg/ mLthrough the induction of apoptosis in MCF-7 breast cancer cell line. Compound **IIIb** has the most antitumor activity (IC_{50} = 16.6 µg/ mL) through the induction of apoptosis in MCF-7 breast cancer cell line, suggesting that it might be a potential alternative agent for human cancer therapy. Compound **IIId** has the lowest antitumor activity with (IC_{50} =19.3µg/ mL) apoptosis in MCF-7 cancer cell line.

Table 1. IC_{50} of the tested compounds on breast cancer.

IC_{50} (µg /mL)	Compound no
Breast cancer	
18.7	**IIIa**
16.6	**IIIb**
18.4	**IIIc**
19.3	**IIId**
18.1	**IIIe**
MCF7-DOX (4.40)	**Standard-DOX**

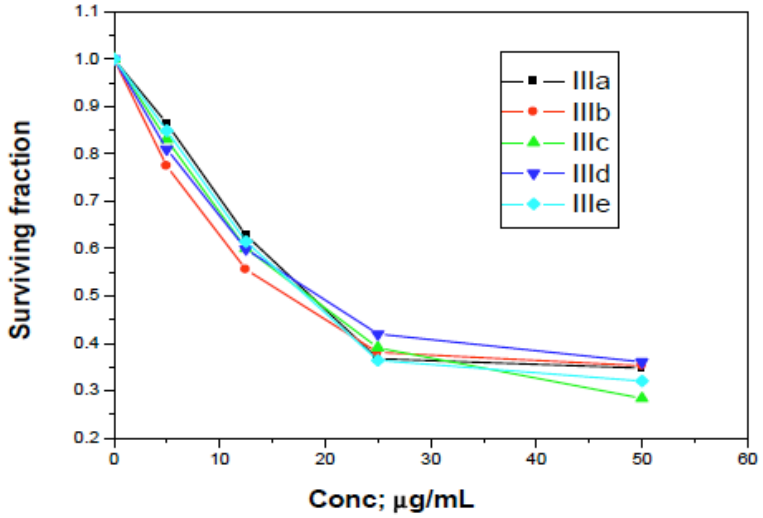

Fig. (1). IC_{50} of the tested compounds on MCF7 for breast cancer.

3. EXPERIMENTAL

3.1. General

Melting points were recorded on a Gallenkamp melting point apparatus and reported uncorrected. The infrared spectra were recorded on Perkin–Elmer FTIR 1430 spectrophotometer using KBr disk technique. The ^{1}H NMR and ^{13}CNMR spectra were recorded on a Bruker AC spectrometer (300 MHz) at 25 °C in DMSO-d_6 with TMS as an internal standard and chemical shifts were reported in ppm as δ values. Reactions were conducted under microwave irradiation in closed vessels under a magnetic stirring in a Synthos 3000 (Anton Paar) microwave with a dual magnetrons system and a maximum power of 1000 W. Mass spectra were measured on a Finnigan MAT 8222 EX mass spectrometer. Microanalyses were performed on Perkin-Elemer 2400 Elemental Analyzer at Micro Analytical Center at Cairo University. Reaction progress was monitored by thin layer chromatography (TLC) using benzene/acetone (2/1 by volume) as eluent. It is worthy to note that compound I was prepared before in another way [25].

3.2. Method (A): Conventional Heating Technique

*4.2.1. Synthesis of 3-(1-methyl-1*H*-imidazol-4-yl)-3-oxopropanenitrile (I)*

To a solution of (0.85 g, 0.01 mole) of cyano acetic acid and 5 ml acetic anhydride, 1-methyl imidazole(0.82 g, 0.01 mole) was added and the reaction mixture was heated at 60-70 ^{o}C with stirring for 10 min. The formed solid was filtrated, dried and crystallized from ethanol to give compounds **I**, M.p. 137-139^{o}C, yield 76%; IR (KBr) υ_{max}/cm^{-1} = 2920 ($CH_{aliphatic}$), 2215 (CN),1690 (C=O),1620 (C=N);^{1}H NMR (300 MHz, DMSO-d6) : δ ppm = 3.47 (s, 2H, CH_2), 3.65 (s, 3H, CH_3), 7.72, 7.91 (s,2H, $H_{imidazole}$), 6.86-7.78 (m, 4H, C_6H_4) ; ^{13}C NMR (75MHz, DMSO-d6):δ ppm = 35.61 (C_1, CH_3), 27 (CH_2), 116 (CN), 132-145(3C, imidazole) 196 (C=O); Anal. Cald. For $C_7H_7N_3O$ (149.15); C, 56.37; H, 4.73; N, 28.17: Found: C, 56.94; H, 5.42; N, 28.54; MS *m/z* 149(M^+).

3.2.2. Synthesis of 1-(4-methoxyphenyl)-3-(1-methyl-1H-imidazol-4-yl)-1H-pyrazol-5-amine (II)

A mixture compound **I** (1.5 g, 0.01 mole) and *p*-anisyl hydrazine hydrochloride (1.7 g, 0.01 mole) was refluxed for 4 h in a 20 ml absolute ethanol. The reaction mixture was evaporated under reduced pressure and the obtained residue was treated with petroleum ether 40-60.The formed solid was filtered, washed with cold ethanol, dried and crystallized from ethyl acetate to give compounds **II**, M.p. 215-217 ^{o}C, yield 72%; IR (KBr) υ_{max}/cm^{-1} = 3327(NH_2), 2896 (CH_{aliph},OCH_3) ,1578 ($C=N_{pyrazol}$);^{1}H NMR (300 MHz, DMSO-d6) : δ ppm = 3.66(s, 3H, CH_3), 3.74 (s, 3H, OCH_3), 4.59 (s,2H, NH_2), 6.75(s, H, $CH_{pyrazole}$), 7.43, 7.98(s, 2H, $H_{imidazole}$), 6.83-7.80 (m, 4H, C_6H_4); ^{13}C NMR (75MHz, DMSO-d6):δ ppm = 40.23 (CH_3N), 55.85 (CH_3O), 97 ($CH_{pyrazol}$), 135-148(3C, imidazole) ; Anal. Cald. For $C_{14}H_{15}N_5O$ (269.32);C,62.44;H,5.61; N, 26.04: Found:C,63.15; H, 6.13;N, 26.34; MS *m/z* 269($M^{+)}$

3.2.3. Synthesis of imidazolyl-pyrazolo[2,3-b]pyridines (IIIa-e)

A mixture of compound **II** (2.7 g, 0.01 mole) and active methylene compounds (0.01 mole), such as ethyl acetoacetate, ethyl benzoylacetate, ethyl cyanoacetate, diethyl malonate, and/or acetyl acetone, was refluxed for (5-8) h in a 10 ml glacial acetic acid. The reaction mixture was cooled, poured on ice/cold water. The formed

Table 2. Experimental data by conventional heating and microwave assisted synthesis.

Comp. No.	Time		Yield (%)	
	Microwave (130°C, min)	Conventional Heating (Reflux,h)	Microwave Irradiation	Conventional Heating
II	20	4	87	72
IIIa	25	5	90	65
IIIb	15	6	92	69
IIIc	15	8	81	72
IIId	15	5	83	65
IIIe	15	5	85	65

solid was filtered, washed with water, dried and crystallized from ethanol to give compounds **IIIa-e**

3.2.3.1. 1-(4-Methoxyphenyl)-4-methyl-3-(1-methyl-1H-imidazol-5-yl)-1H-pyrazolo[3,4-b] pyridin-6-ol (III$_a$)

M.p. 214-216°C, yield 65%; %; IR (KBr) υ_{max}/cm^{-1} = 3412(OH), 2954 (CH_{aliph},OCH_3) ,1607 ($C=N_{pyrazol}$);^{1}H NMR (300 MHz, DMSO-d6): δ ppm = 2.56 (s,3H,$CH_{3pyridine}$), 3.48 (s, 3H, CH_3),3.67(s,3H,OCH_3), 5.26 (s,H,OH), 6.80 (s, H,$CH_{pyridine}$), 7.32, 7.87 (s, 2H, $H_{imidazole}$), 6.88-7.89 (m, 4H, $H_{aromatic}$); ^{13}C NMR (75MHz, DMSO-d6):δ ppm = 35.6 (CH_3N), 52.15 (CH_3O), 89.43($CH_{pyrazol}$), 135-146(3C, $_{imidazole}$) ; Anal. Cald. For $C_{18}H_{17}N_5O_2$ (335.16); C, 64.47; H, 5.11; N, 20.88: Found: C, 64.93; H, 5.62; N, 21.14; MS *m/z* 335(M^+).

3.2.3.2. 1-(4-Methoxyphenyl)-3-(1-methyl-1H-imidazol-4-yl)-6-phenyl-1H-pyrazolo[3,4-b] pyridin-4-ol. (III$_b$)

M.p. 244-246 °C, yield 69%; %; IR (KBr) υ_{max}/cm^{-1} = 3411(OH),3055($CH_{aromatic}$) 2897 (CH_{aliph}, OCH_3) ,1632($C=N_{pyrazol}$); ^{1}H NMR (300 MHz, DMSO-d6): δ ppm =3.54(s,3H, CH_3), 3.67(s, 3H,OCH_3), 5.46 (s,H, OH), 6.48, 7.20 (s, 2H,H $_{imidazole}$), 6.80 (s, H,$CH_{pyridine}$), 7.42-7.75(m,9H,$H_{aromatic}$); ^{13}C NMR (75MHz, DMSO-d6):δ ppm = 36.78(CH_3N), 51.32 (CH_3O), 92.6 ($C_{,pyrazol}$), 135-149(3C, $_{imidazole}$), 130-156(3$C_{pyridine}$) ; Anal. Cald. For $C_{23}H_{19}N_5O_2$ (397.17); C, 69.51; H, 4.83; N, 17.62: Found: C, 70.11; H, 5.22; N, 17.94; MS *m/z* 397(M^+).

3.2.3.3. 6-Amino-1-(4-methoxyphenyl)-3-(1-methyl-1H-imidazol-4-yl)-1H-pyrazolo[3,4-b] pyridin-4-ol (IIIc)

M.p. 189-192 °C, yield 72%; %; IR (KBr) υ_{max}/cm^{-1} = 3376 (OH), 3110($CH_{aromatic}$), 2924(CH_{aliph}, OCH_3), 1621($C=N_{pyrazol}$); ^{1}H NMR (300 MHz, DMSO-d6): δ ppm =3.64(s,3H, CH_3),3.75 (s, 3H, OCH_3 $_{imidazole}$) ,4.19 (s,2H,NH_2), 5.46 (s, H, OH), 6.94, 7.31 (s, 2H,H $_{imidazole}$), 6.94 (s, H, $H_{pyridine}$), 6.85-7.45(m, 4H, $H_{aromatic}$).

^{13}C NMR (75MHz, DMSO-d6):δ ppm = 36.52(CH_3N), 53.74 (CH_3O), 89.36 ($C_{,pyrazol}$), 132-149(3C, $_{imidazole}$),125-156(3$C_{pyridine}$) ; Anal. Cald. For $C_{17}H_{16}N_6O_2$ (336.17); C, 60.71; H, 4.79; N, 24.99: Found: C, 60.93; H, 5.02 ;N, 25.21; MS *m/z* 336(M^+).

3.2.3.4. 1-(4-Methoxyphenyl)-3-(1-methyl-1H-imidazol-4-yl)-1H-pyrazolo[3,4-b]pyridine-4,6-diol (IIId)

M.p. 214-216 °C, yield 65%; %; IR (KBr) υ_{max}/cm^{-1} = 3435(OH), 3092($CH_{aromatic}$), 2944(CH_{aliph}, OCH_3), 1598 ($C=N_{pyrazol}$); ^{1}H NMR (300 MHz, DMSO-d6): δ ppm =3.68 (s, 3H, CH_3 $_{imidazole}$), 3.71(s,3H,OCH_3), 5.37, 5.42(s, 2H, 2OH), 6.46, 7.30 (s, 2H,H $_{imidazole}$), 6.51(s, H, $H_{pyridine}$), 6.78-7.36(m,4H,$H_{aromatic}$); ^{13}C NMR (75MHz, DMSO-d6):δ ppm = 14.8, 28.7(2CH_3 $_{imidazole}$), 48.74 (CH_3O), 88.34 ($C_{,pyrazol}$), 124-138(3C, $_{imidazole}$), 136-155(3$C_{pyridine}$) ; Anal. Cald. For $C_{17}H_{15}N_5O_3$ (337.15); C, 60.53; H, 4.48; N, 20.76: Found: C, 60.88; H, 4.85; N, 21.26; MS *m/z* 337(M^+).

4.2.3.5. 1-(4-Methoxyphenyl)-4,6-dimethyl-3-(1-methyl-1H-imidazol-4-yl)-1H-pyrazolo[3,4-b]pyridine (IIIe)

M.p.234-236 °C, yield 65%; %; IR (KBr) υ_{max}/cm^{-1} =3123 ($CH_{aromatic}$), 2950 (CH_{aliph}, OCH_3, $2CH_3$), 1604($C=N_{pyrazol}$); ^{1}H NMR (300 MHz, DMSO-d6): δ ppm =2.35, 3.46 (s, 6H,2$CH_{3pyridine}$), 3.58 (s, 3H, CH_3), 3. 68 (s,3H,OCH_3),7.18 (s,H,$H_{pyridine}$), 6.82-7.25 (m,4H,H_{arom}); ^{13}C NMR (75MHz, DMSO-d6): δ ppm = 23.5, 27.4(2CH_3 $_{pyridine}$), 38.2($CH_{3,imidazole}$), 53.54 (CH_3O), 114-145(3C, $_{aromatic}$); Anal. Cald. For $C_{19}H_{19}N_5O$ (333.16); C, 68.43; H, 5.74; N, 21.02 Found: C, 68.94; H, 6.02; N, 21.46; MS *m/z* 333(M^+).

3.3. Method (B): Microwave Irradiation Techniques

The procedure was similar to that described in method (A) except that the mixture was capped in a closed vessel and irradiated in a microwave oven at 130-150 °C for the mentioned time. The reaction mixture was worked up as usual to give **compounds II** and **IIIa-e** (Table **2**).

4. COMPUTATIONAL DETAILS:

4.1. Quantum Chemical Calculations

Full-unconstrained geometry optimizations of the investigated compounds were carried out at a gradient corrected DFT using Becke's three parameter hybrid method and Lee–Yang–Parr correlation functional (B3LYP) [26] combined with 6-31+G(d) basis set [27] using Gaussian 09 [28] in the gas phase. Frequency calculations showed that all structures have stationary points in the geometry optimization procedures with no imaginary frequencies in the vibrational analyses, indicating minimal energy structures.

The optimized geometry of the studied molecules, molecular frontier orbitals HOMO (highest occupied molecular orbital), LUMO (lowest unoccupied molecular orbital) and the molecular electrostatic potential (MEP) were visualized with ChemCraft program [29] and Gaussian View [30] respectively.

4.2. Molecular Docking Simulation

The computational study was carried out on Hp-pc (Hp pavilion dv6 Notebook pc) with AMD phenom (tm) II N930 Quad-Core processor 2.00 GHZ and RAM is 4.00 GB. Docking simulation was performed using Molegro Virtual Docker (MVD) [31, 32] a program for predicting the most likely conformation of how a ligand will bind to a macromolecule. This study began with the examination of known structure for cathepsin D obtained from the protein data bank (PDB code 4OBZ with resolution 2.9 Å). The native ligand was removed from the active site and redocked into the binding site of its enzyme in order to characterize the binding pocket of

Table 3. The calculated quantum chemical parameters obtained from DFT B3LYP/ 6-31g+ (d). For the investigated compounds.

Molecule	E_{HOMO} (eV)	E_{LUMO} (eV)	ΔE (eV)	μ (D)	A (eV)	I (eV)	η (eV)	σ (eV^{-1})	χ (eV)	Pi (eV)	ω (eV)	*log p*	*M.V*
IIIa	**-5.163**	**-1.209**	**3.954**	**6.261**	**1.209**	**5.163**	**1.977**	**0.506**	**-3.186**	**3.186**	**2.567**	**1.500**	**959.390**
IIIb	**-5.233**	**-1.579**	**3.654**	**5.687**	**1.579**	**5.233**	**1.827**	**0.547**	**-3.406**	**3.406**	**3.175**	**2.930**	**1118.400**
IIIc	**-5.199**	**-1.112**	**4.088**	**7.766**	**1.112**	**5.199**	**2.044**	**0.489**	**-3.156**	**3.156**	**2.436**	**1.520**	**926.660**
IIId	**-5.185**	**-1.357**	**3.828**	**6.070**	**1.357**	**5.185**	**1.914**	**0.523**	**-3.271**	**3.271**	**2.795**	**2.250**	**982.880**
IIIe	**-5.056**	**-0.849**	**4.207**	**6.672**	**0.849**	**5.056**	**2.104**	**0.475**	**-2.953**	**2.953**	**2.073**	**0.23**	**941.890**

the enzyme (the grid dimensions were; x= -33.17, y= 0.48 and z= -12.86 Å, and the radius is 15 Å).

5. RESULTS AND DISCUSSION

5.1. Quantum Chemical Descriptors

For understanding various aspects of pharmacological science including drug design and the possible eco-toxicological characteristics of the drug molecules, several new chemical reactivity descriptors have been proposed. Conceptual DFT based descriptors have helped in many ways to understand the electronic structure of the molecules and their reactivity by calculating the energy of the highest occupied molecular orbital (E_{HOMO}), the energy of the lowest unoccupied molecular orbital (E_{LUMO}), the energy gap ΔE, (E_{LUMO}-E_{HOMO}), the dipole moment (μ), ionization potential (Pi), electron affinity (A), electronegativity (χ), chemical potential (Pi), the hardness (η), the softness (σ), the electrophilicity index (ω), lipophilicity (log p) and the molecular volume (MV),which are proved to be useful quantities in chemical reactivity theory, Table **3**.

Experimentally, the compound (**IIIb**) showed the highest biological activity, while the compound (**IIId**) had the lowest one among the investigated compounds. Accordingly, quantum chemical calculations were performed using DFT/B3LYP/6-31G +(d,p) to explain the effect of electronic and structural parameters on the efficiency of the studied compounds and try to find a correlation with the experimental results to predict the mode of interaction of these inhibitors with the enzyme.

The calculations showed that the compound (**IIIb**) with substituted phenyl group at pyrazolo-pyridine moiety has the lowest LUMO energy (-1.579 eV) and accordingly the highest EA (1.579eV) among the investigated inhibitors (Table **3**), which could probably increase its ability to be attacked by nucleophile. This means that the compound (**IIIb**) is able to form a hydrogen bond interaction with the enzyme and accordingly increases its efficacy.

HOMO-LUMO energy gap (ΔE) is an important stability index, which is applied to develop a theoretical model for explaining the structure and conformation barriers in many molecular systems. The calculations showed that inhibitor **(IIIb)** has the lowest separation energy, ΔE, (3.654 eV), which could explain its highest reactivity towards the enzyme comparing with the rest of compounds which is in a good agreement with the experimental observation.

Absolute hardness, η, and softness, σ, are important properties to measure the molecular stability and reactivity. Soft molecules are reactive because they easily offer electrons to an acceptor. The calculations indicated that the presence of phenyl group in compound (**IIIb**) increases its global softness, (0.547 eV^{-1}), which probably leads to improve its inhibition efficiency. It was shown from the calculation that the inhibitor (**IIIb**) has the highest electronegativity and chemical potential (-3.186 and 3.186 eV), respectively, (Table **3**) which could decrease its electron donating ability (lower oxidized) compared with the other investigated compounds.

The polar molecules dissociate better than non-polar molecules whereby the polarity of the molecule is generally expressed in terms of dipole moment (DM). It is a physicochemical property of a drug candidate which is widely used in the medicinal chemistry as an index of lipophilicity and ability of drug molecule for crossing various biological membranes. The calculations showed that the inhibitor (**IIIb**) has the lowest dipole moment value (5.687D) among the studied molecules, Table **1**. This means that this inhibitor is the most lipophilic one which is confirmed from the calculated lipophilicity index log p. The more the values of log p, the more hydrophobicity, and the calculations showed that the inhibitor (**IIIb**) has the highest log p value (2.930) among the studied inhibitors, which indicated the importance of the presence of phenyl substituent to accelerate the rate of diffusion across the membrane thereby showing a considerable anticancer effect.

Electrophilicity index encompasses both the ability of an electrophile to acquire additional electronic charge and the resistance of the system to exchange electronic charge with the environment. It was shown from the calculations that the compound (**IIIb**) has the highest electrophilicity index (3.175), which could explain its highest biological activity.

It was concluded from the above discussion that the calculated quantum chemical parameters confirmed that the compound (**IIIb**) with phenyl substituent at position 6 in pyrazolopyridine moiety showed the highest biological activity comparable with the other inhibitors, which agrees well with the experimental observation.

Also, it was found from the experimental results that the presence of methyl group at position 6 in the pyrazolopyridine moiety enhances the biological activity comparing with hydroxyl group at the same position, (compounds **IIIa** and **IIId**), respectively. The calculations showed that the presence of methyl group, compound (**IIIa**) decreases the E_{LUMO}, ΔE and μ (-5.163eV, 3.954 eV and 6.261D), respectively, compared with compound (**IIId**) (-5.199eV, 4.088 eVand 7.766 D), respectively, Table **3**, which probably leads to increase its potency. Also, the calculations showed that the presence of alkyl group increases the E_{HOMO} by about 0.036 eV with respect to the hydroxyl group, which enhances the donation ability of compound (**IIIa**) towards the enzyme, which explains its biological activity. The calculations showed that the compound (**IIIa**) has higher σ, ω and Pi (0.506 eV^{-1}, 2.567and 3.186eV), respectively, than those of compound (**IIId**) (0.489 eV^{-1}, 2.436 and 3.156 eV), respectively, Table **3**. According to the calculated quantum chemical parameters the presence of methyl group seems to be better than the hydroxyl one for enhancing the biological activity which agrees well with the experimental observation.

Experimentally, the presence of two methyl groups at positions 4 and 6 in pyrazolopyridine moiety (**IIIe**) is more biologically favored than the two hydroxyl groups at the same position (**IIId**) which is confirmed from the quantum chemical calculations. The presence of methyl groups increases the E_{HOMO} to be (-5.185 eV) and decreases the E_{LUMO}, ΔE and μ by about (0.245, 0.260 eVand 1.696 D), respectively, which leads to improve the potency of com-

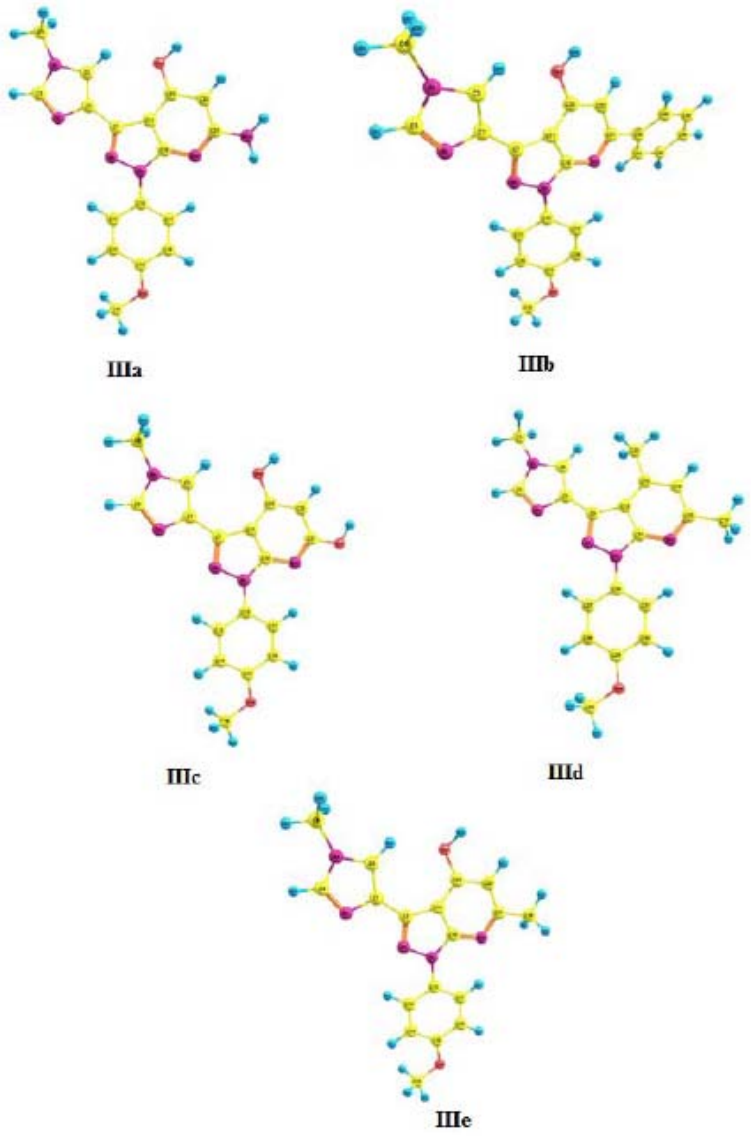

Fig. (2). The optimized molecular structures of the investigated compounds.

pound (**IIIe**) with respect to compound (**IIId**). Also, the calculations showed that the two methyl group increase the values of log p, σ, ω, pi and A to be (2.250, 0.523 eV^{-1}, 2.795, 3.271 eV and 1.357 eV), respectively, Table **3**, which are responsible for the increasing of the biological activity of compound (**IIIe**) with respect to inhibitor (**IIId**).

The optimized molecular structures with the minimum energies obtained from the quantum chemical calculations are shown in Fig. (**2**).

5.2. Frontier Molecular Orbital and Molecular Reactivity

To explain several types of reaction and for predicting the most reactive sites in conjugated systems, molecular orbitals and their properties such as energy were calculated. The calculations showed that all tested compounds have similar charge density distribution at the HOMO level, Fig (**3**). The charge is localized over the whole skeleton of the molecules which explains the reactivity of the investigated compounds. Also, the charge density of the LUMO level is almost delocalized on pyrazolo-pyridine moiety for all investigated inhibitors, Fig. (**3**), which means that they will be reacted as electrophile (electron acceptor). This explains the role of the substituents on the pyrazolo-pyridine moiety for future drug design.

5.3. Molecular Electrostatic Potential (MEP)

Molecular electrostatic potential (MEP) map is a very useful descriptor in understanding sites for electrophilic attack, nucleophilic reactions for the study of biological recognition process and hydrogen bonding interactions [33]. The color-coded maps region given as red or orange represent the areas with high electron density, whereas the blue areas represent electron poor sites. In order to predict the molecular reactive sites, MEP was calculated. One can observe that the most negative potential on all investigated inhibitors was ascribed to the nitrogen atoms and oxygen atom of methoxy group. On the other hand, all investigated drugs have highly electron deficient on their whole skeleton which have described as essential to hydrogen bond with the active site of cathepsin D, as shown in Fig (**4**). The moieties with positive electrostatic potentials bind deeply into the negative electrostatic potential of the active site while the atoms with the negative electrostatic potentials bind to a positive part of the active site, which might be important to generate an ideal docking pose of the drug within the binding pocket. This study revealed that the catalytic active site of the target enzyme has a negative electrostatic potential which was complemented with a positive electrostatic potential of the investigated inhibitors to form a stabilized complex.

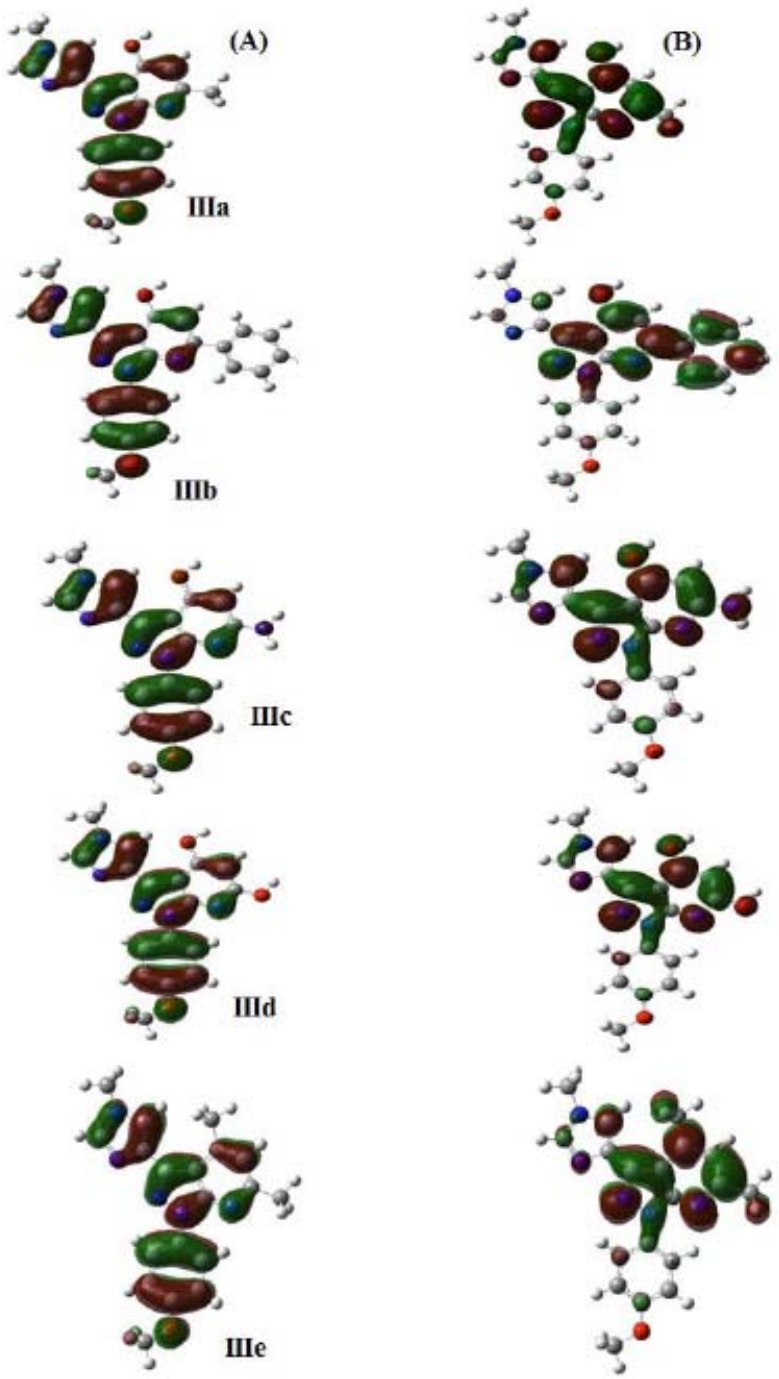

Fig. (3). The charge density distribution of frontier molecular orbitals HOMO (A) and LUMO (B).

It was concluded from the above that the quantum chemical parameters confirmed with MEPs are able to describe the biological activity of compounds.

5.4. Structure Activity Relationship (SAR)

The aim of the present SAR study is to have a correlation between the biological activities of the investigated compounds with the most effective quantum chemical descriptors. Different descriptors such as E_{LUMO}, lipophilicity descriptor (Log p), dipole moment, energy gap (ΔE), electrophilicity (ω), softness, chemical potential and the molecular volume (MV) were correlated well with the experimental biological activity and have high correlation coefficient. Fig. (**5**). shows some representative plots of the correlations between the above quantum chemical parameters and experimental IC_{50}. It was concluded from SAR analysis that the electronic, spatial and fast descriptors are very useful tools for a better description of the potency of the tested compounds and good prediction for new potent anticancer drug.

5.5. Molecular Docking Analysis for the Most Potent Inhibitor (IIIb)

Cathepsin D is an aspartyl peptidase, founded in a wide variety of cell and tissue types [34] which is important in several physiological and pathophysiological processes. Cathepsin D has recently been of interest in cancer research because of its putative role in the progress of cancer formation [35-38]. Cathepsin D activity has been

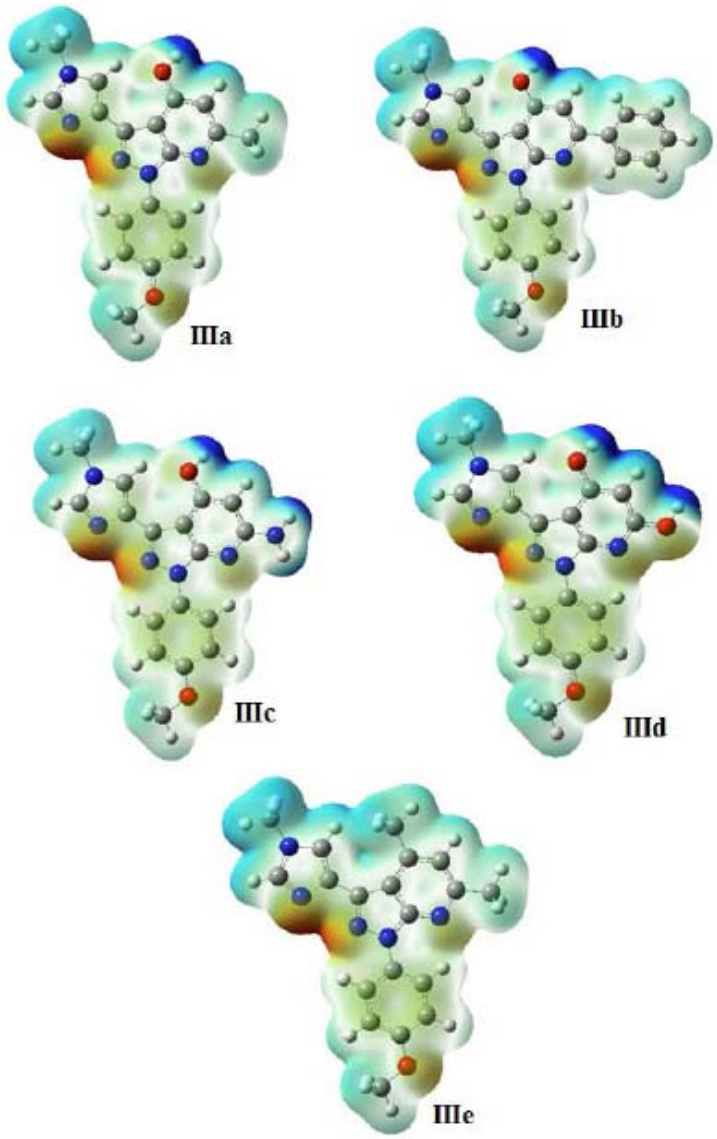

Fig. (4). Molecular electrostatic potential for all optimized structures of the investigated inhibitors.

used as a predictive marker for diagnosis of breast cancer [39, 40]. Cathepsin D is also expressed in human breast cancer MCF-7 cell; estrogen receptor-positive cells [41]. Expression of Cathepsin D in cultured MCF-7 has also become a marker for assay of the estrogenic activity of environmental chemicals, because Cathepsin D can be induced by estrogen in MCF-7 cells [42].

It is important to mention that the conformational analysis has been carried out for all rotatable bonds of the inhibitor (**IIIb**) in order to correctly evaluate the conformational space of the title inhibitor and the dihedral angles which cause important steric effects and also, to get the information about putative minima obtained through the conformational search. The optimized molecular structure of inhibitor1-(4-methoxyphenyl)-3-(1-methyl-1H-imidazol-4-yl)-6-phenyl-1H-pyrazolo[3,4-*b*]- pyridine-4-ol (**IIIb**) was used as input file for the conformational analysis carried out with conformational search method implemented in material studio 4.3 software package [43]. The molecular structure of the lowest energy conformer for the investigated compound is shown in Fig. (**S1**). The lowest energy conformer was used for the docking calculations.

Molecular modeling and molecular docking studies were performed on one of the most potent inhibitor, (**IIIb)**, among our investigated drugs in order to determine the binding mode and understand the mode of interaction of (**IIIb**) inhibitor and Cathepsin D. The calculations of the interaction between inhibitor (**IIIb**) and Cathepsin D binding pocket showed that there are four hydrogen bond interactions with the important amino acid residues:Tyr205 (2.83Å and 3.42Å), Asp231 (2.01 Å) and Thr234 (2.83 Å). These interactions enhance the stabilization of Cathepsin D and inhibitor (**IIIb**), Fig. (**6**). Additionally, the substituted phenyl moiety at position 6 of (**IIIb**) nucleus plays an important role for its interaction with the lipophilic pocket of the enzyme. The docking calculations showed that the phenyl moiety forms a van der Waals interaction with Tyr78 residue with a distance (3.86 Å). It seems that these kinds of interactions are probably responsible for the stabilization of protein inhibitor complex, as shown in Fig. (**S2**) and Fig. (**7**). The electrostatic map contribution of protein with (**IIIb**) ligand complex, Fig. (**S3**) showed that the binding groove of cathepsin D has negative electrostatic potential and the inhibitor (**IIIb**) has positive electrostatic potential. This may be one of the structural reasons for a higher activity of this molecule. It was concluded from the above discussion that the substituted phenyl moiety at position 6 increases the inhibitory potency, which agrees well with the experimental observations.

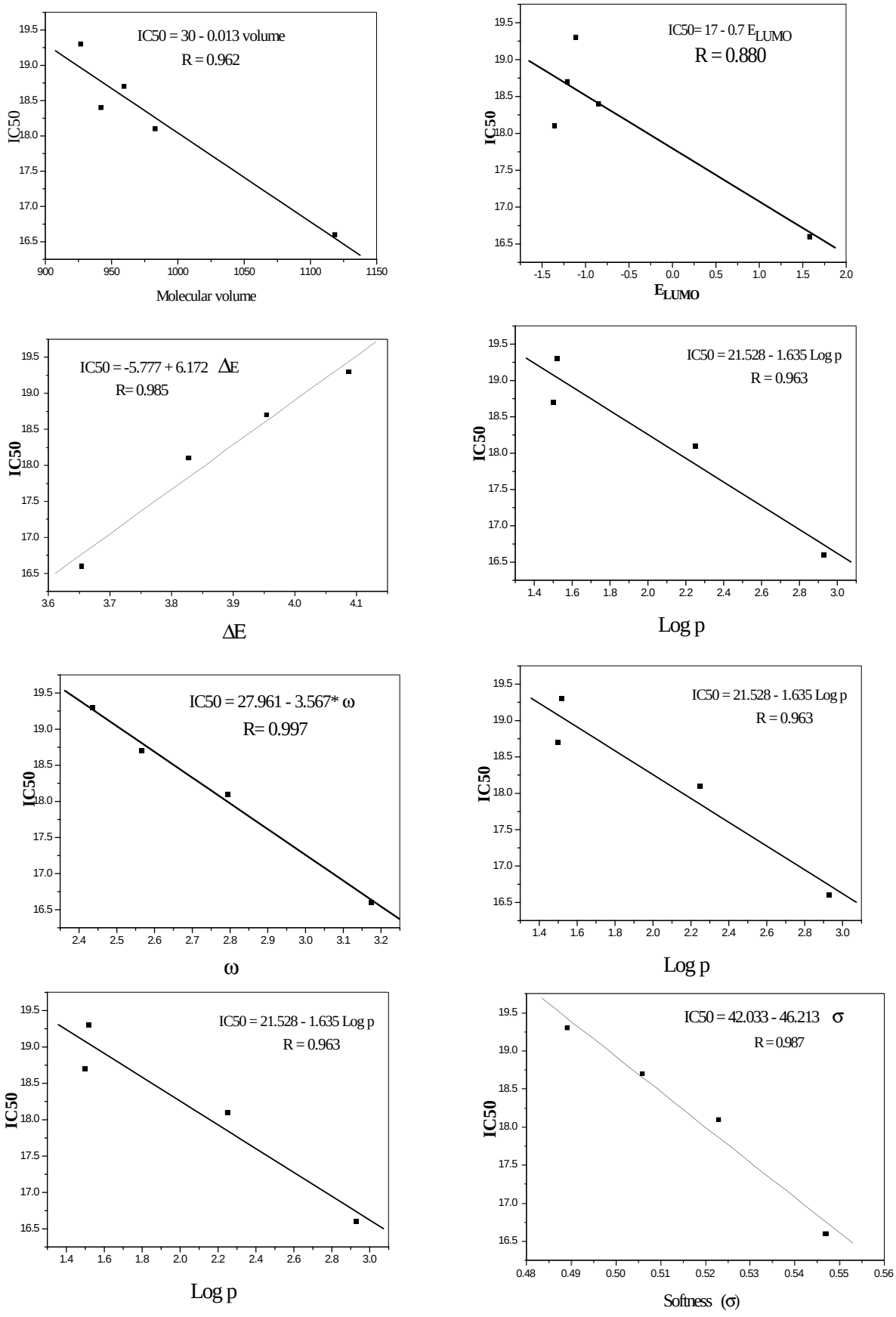

Fig. (5). Linear correlation between experimental biological activity (IC_{50}) and quantum chemical descriptors for the investigated anticancer inhibitors.

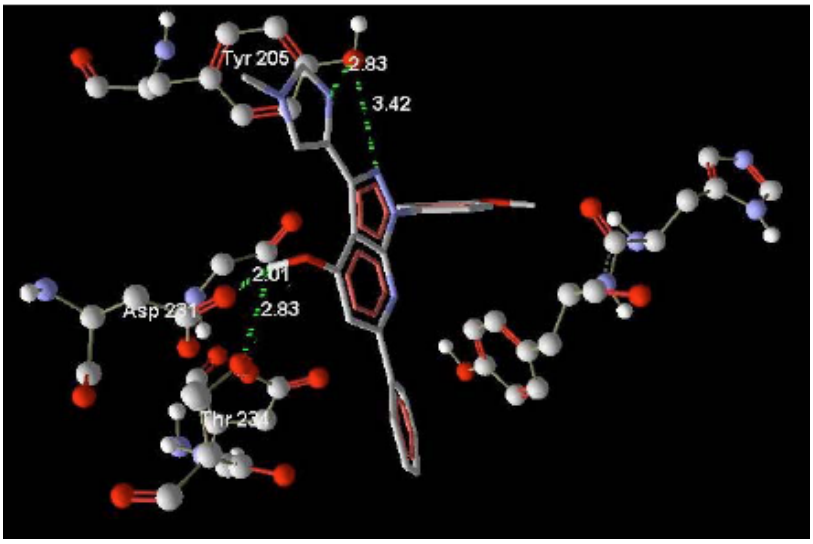

Fig. (6). Putative binding modes and molecular interactions of IIIb in the active site of Cathepsien D. Hydrogen bond interactions are indicated by dotted lines, with numerals indicating distance in angstroms. Protein is represented by sticks and (**IIIb**) is represented by balls and sticks.

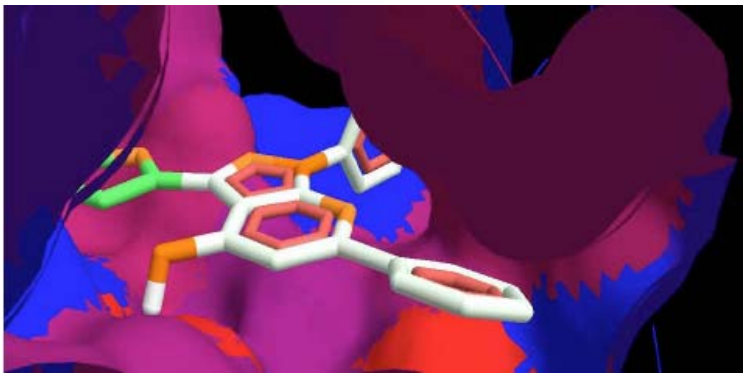

Fig. (7). Surface representation of the hydrophobic pocket of Cathepsin D with the docked compound (**IIIb**).

CONCLUSION

The objective of this work was established in vitro antiproliferative activities against MCF-7 (breast cancer) human cell lines for of the synthesized compounds **IIIa-e**. The quantum chemical descriptors confirmed that inhibitor1-(4-methoxyphenyl)-3-(1-methyl-1*H*-imidazol-4-yl)-6-phenyl-1*H*-pyrazolo[3,4-b]- pyridine-4-ol (**IIIb**) is the most potent and reactive among the investigated compounds. This conclusion is congruent with the results obtained experimentally.

ETHICS APPROVAL AND CONSENT TO PARTICIPATE

Not applicable.

HUMAN AND ANIMAL RIGHTS

No Animals/Humans were used for studies that are base of this research.

CONSENT FOR PUBLICATION

Not applicable.

CONFLICT OF INTEREST

The authors declare no conflict of interest, financial or otherwise.

ACKNOWLEDGEMENTS

Authors would like to Acknowledge Prof. James Gauld, Windsor University, Canada, for using Orca.net.ca to do our calculations.

SUPPLEMENTARY MATERIAL

Supplementary material is available on the publisher's web site along with the published article.

REFERENCES

[1] Brogden, R.N.; Heel, R.C.; Speight, T.M.; Avery, G.S. Metronidazole in anaerobic infections: a review of its activity, pharmacokinetics and therapeutic use. *Drugs*, **1978**, *16*, 387-396.

[2] di Santo, R.; Tafi, A.; Costi, R.; Botta, M.; Artico, M.; Corelli, F.; Forte, M.; Caporuscio, F.; Angiolella, L.; Palamara, A.T. Antifungal agents. 11. N-substituted derivatives of 1-[(Aryl)(4-aryl-1H-pyrrol-3-yl)methyl]-1H-imidazole: Synthesis, anti-candida activity, and QSAR studies. *J. Med. Chem.*, **2005**, *48*, 5140-5152.

[3] Brimblecombe, R.W.; Duncan, W.A.M.; Durant, G.J.; Emmett, Ganellin, J.C.; C.R.; Parsons, M.E.; Cimetidine—A Non-Thiourea H2-Receptor Antagonist. *J. Int. Med. Res.*, **1975**, *2*, 86-92.

[4] Pathan, M.Y.; Paike, V.V.; Pachmase, P.R.; More, S.P.; Ardhapure, S.S.; Pawar, R.P. Microwave-assisted facile synthesis of 2-substituted 2-imidazolines. *Arkivoc*, **2006**, *15*, 205-210.

[5] Elnagdi, M.H.; Fahmy, S.M.; Hafez, E.A.; Elmoghayar, A.; Amer, S.A.R. Pyrimidine derivatives and related compounds: A novel synthesis of pyrimidines, pyrazolo[4,3-d] pyrimidines, and isoxazolo[4,3-d] pyrimidines. *J. Heterocycl. Chem.*, **1979**, *16*, 1109.

[6] Aggarwal, R.; Singh, G.; Kaushik, P.; Kaushik, D.; Paliwal, D.; Kumar, A. Molecular docking design and one-pot expeditious synthesis of novel 2,5-

diarylpyrazolo[1,5-a]pyrimidin-7-amines as anti-inflammatory agents. *Eur. J. Med. Chem.*, **2015**, *101*, 326-333.

[7] Elnagdi, M.H.; Khalifa, M.A.; Ibraheim, A.K.; Elmoghayar, M.R. The reaction of nitriles with mercaptoacetic acid: A new synthesis of thiazole derivatives. *J. Heterocycl. Chem.*, **1981**, *18*, 877-879.

[8] Wenglowsky, S.; Ahrendt, K.A.; Buckmelter, A.J.; Feng, B.; Gloor, S.L.; Gradl, S.; Grina, J.; Hansen, J.D.; Laird, E.R.; Lunghofer, P.; Mathieu, S.; Moreno, D.; Newhouse, B.; Ren, L.; Risom, T.; Rudolph, J.; Seo, J.; Sturgis, H.L.; Voegtli, W.C.; Wen, Z. Pyrazolopyridine inhibitors of B-RafV600E. Part 2: structure-activity relationships. *Bioorg. Med. Chem. Lett.*, **2011**, *18*, 5533-5537.

[9] Quiroga, J.; Portilla, J.; Insuasty, B.; Abnia, R.; Nogueras, M.; Sortino, M.; Zacchino, S. Solvent-free microwave synthesis of bis-pyrazolo[3,4-b:4',3'-e]pyridines and study of their antifungal properties. *J. Heterocycl. Chem.*, **2005**, *42*, 61-66.

[10] Abu-Hashem, A.A.; Gouda, M.A. Synthesis, anti-inflammatory and analgesic evaluation of certain new 3a,4,9,9a-tetrahydro-4,9-benzenobenz[f]isoindole-1,3-diones. *Arch. Pharm. (Weinheim)*, **2011**, *344*(8), 543-551.

[11] Löwe, W.; Braun, B.; Müller, B. Novel pyranopyridine derivatives from an enaminone. *J. Heterocycl. Chem.*, **1994**, *31*, 1577-1581.

[12] Hassaneen, H.M. Chemistry of the enaminone of 1-acetylnaphthalene under microwave irradiation using chitosan as a green catalyst. *Molecules*, **2011**,*16*, 609-623.

[13] Tuccinardi, T.; Zizzari, A.T.; Brullo, C.; Daniele, S.; Musumeci, F.; Schenone, S.; Trincavelli, M.L.; Martini, C.; Martinelli, A.; Giorgi, G.; Botta, M. Substituted pyrazolo[3,4-b]pyridines as human A1 adenosine antagonists: developments in understanding the receptor stereoselectivity. *Org. Biomol. Chem.*, **2011**, *9*, 4448-4455.

[14] Dipti, K.D.; Amit, R.T.; Vipul, B.K.; Viresh, H.S. Advances in the synthesis of pyrazolo[3,4-b]pyridines. *Curr. Org. Chem.*, **2012**, *16*, 400-417.

[15] Patil, S.G.; Bhadke, V.V.; Bagul, R.R. Synthesis of pyrazolo [3,4-b] pyridines using basic ionic liquid [bmIm]OH. *J. Chem. Pharm. Res.*, **2012**, *4*, 2751-2754.

[16] El-borai, M.A.; Rizk, H.F.; Abd-Aal, M.F.; El-Deeb, I.Y. Synthesis of pyrazolo[3,4-b]pyridines under microwave irradiation in multi-component reactions and their antitumor and antimicrobial activities - Part 1. *Eur. J. Med. Chem.*, **2012**, *48*, 92-96.

[17] M.A. El-Borai, H.F. Rizk, D.M. Beltagy, I.Y. El-Deeb, *Eur. J. Med. Chem.*, **2013**,66, 415-422.

[18] El-Borai, M.A.; Rizk, H.F.; El-Deeb, I.Y.; Sadek, M.E. A convenient synthesis of a series of pyrazolo[3,4-d]pyrimidines as potential antimicrobial and antioxidant agents. *J. Appl. Chem (JOAC)*, **2014**, *4*, 1526-1537.

[19] Zhou, T.; Huang, D.Z.; Caflisch, A. Quantum mechanical methods for drug design. *Curr. Top. Med. Chem.*, **2010**, *10*, 33-45.

[20] Raha, K.; Peters, M.B.; Wang, B.; Yu, N.; Wollacott, A.M.; Westerhoff, L.M.; Merz, K.M.Jr. The role of quantum mechanics in structure-based drug design. *Drug Discov. Today*, **2007**, *12*, 725-731.

[21] Demain, A.L.; Sanchez, S.J. Microbial drug discovery: 80 years of progress. *J. Antibiot. (Tokyo)*, **2009**, *62*(1), 5-16.

[22] ~~C.W. Perry, B.J. Phillips, Int. J. Oncol., **2002**, 1, 1-5.~~

[23] Jemal, A.; Bray, F.; Center, M.M.; Ferlay, J.; Ward, E.; Forman, D. Global cancer statistics. *CA Cancer J. Clin.*, **2011**, *61*(2), 69-90.

[24] Skehan, P.; Storeng, R.; Scudiero, D.; Monks, A.; McMahon, J.; Vistica, D.; Warren, J.T.; Bokesch, H.; Kenney, S.; Boyd, M.R. New colorimetric cytotoxicity assay for anticancer-drug screening. *J. Natl. Cancer Inst.*, **1990**, *82*(13), 1107-1112.

[25] Al-Matar, H.M.; Khalil, K.D.; Al-Kanderi, M.F.; Elnagdi, M.H. Studies on 3-oxoalkanenitriles: novel rearrangement reactions observed in studies of the chemistry of 3-heteroaroyl-3-oxoalkanenitriles as novel routes to 2-dialkylaminopyridines. *Molecules*, **2012**, *17*(1), 897-909.

[26] Becke, A.D. Density-functional thermochemistry. III. The role of exact exchange. *J. Chem. Phys.*, **1993**, *98*, 5648-5652.

[27] Hay, P.J.; Wadt, W.R. *Ab initio* effective core potentials for molecular calculations. Potentials for K to Au including the outermost core orbitals. *J. Chem. Phys.*, **1985**, *82*, 270-285.

[28] Frisch, M.J.; Trucks, G.W.; Schlegel, H.B.; Scuseria, G.E.; Robb, M.A.; Cheeseman, J.R.; Scalmani, G.; Barone, V.; Mennucci, B.; Petersson, G.A.; Nakatsuji, H.; Caricato, M.; Li, X.; Hratchian, H.P.; Izmaylov, A.F.; Bloino, J.; Zheng, G.; Sonnenberg, J.L.; Hada, M.; Ehara, M.; Toyota, K.; Fukuda, R.; Hasegawa, J.; Ishida, M.; Nakajima, T.; Honda, Y.; Kitao, O.; Nakai, H.; Vreven, T.; Montgomery, J.A.; Peralta, J.E.; Jr., Ogliaro, F.; Bearpark, M.; Heyd, J.J.; Brothers, E.; Kudin, K.N.; Staroverov, V.N.; Keith, T.; Kobayashi, R.; Normand, J.; Raghavachari, K.; Rendell, A.; Burant, J.C.; Iyengar, S.S.; Tomasi, J.; Cossi, M.; Rega, N.; Millam, J.M.; Klene, M.; Knox, J.E.; Cross, J.B.; Bakken, V.; Adamo, C.; Jaramillo, J.; Gomperts, R.; Stratmann, R.E.; Yazyev, O.; Austin, A.J.; Cammi, R.; Pomelli, C.; Ochterski, J.W.; Martin, R.L.; Morokuma, K.; Zakrzewski, V.G.; Voth, G.A.; Salvador, P.; Dannenberg, J.J.; Dapprich, S.; Daniels, A.D.; Farkas, O.; Foresman, J.B.; Ortiz, J.V.; Cioslowski, J.; Fox, D.J. Gaussian, Inc., Wallingford CT, 2010. Gaussian 09, Revision C.01.

[29] Zhurko, G.A. Chemcraft V1.6, http://www.Chemcraftptrog.Com.

[30] Dennington II, R.; Keith, T.; Millam, J. Gauss View, Version 4.1.2, Semichem Inc., Shawnee Mission, KS, **2007**.

[31] Molegro Virtual Docker **2008**. http://www.molegro.com/mvd-product.php.

[32] Thomsen, R.; Christensen, M.H. MolDock: a new technique for high-accuracy molecular docking. *J. Med. Chem.*, **2006**, *49*(11), 3315-3321.

[33] Rodrigues, T.; Daniel, J.V.A.; Santos, D.; Moreira, R.; Lopes, F.; Guedes, R.C. A quantum mechanical study of novel potential inhibitors of cytochrome bc$_1$ as antimalarial compounds. *Int. J. Quant. Chem.*, **2011**, *111*, 1196-1211.

[34] Fusek, M.; Vetvucka, V. *Aspartic Proteinases, Physiology and Pathology*, CRC Press: New York, **1995**.

[35] Mordente, J.A.; Choudhury, M.S.; Tazaki, H.; Mallouh, C.; Konno, S. Hydrolysis of androgen receptor by cathepsin D: Its biological significance in human prostate cancer. *Br. J. Urol.*, **1998**, *82*(3), 431-435.

[36] Leto, G.; Gebbia, N.; Rausa, L.; Tumminello, F.M. Cathepsin D in the malignant progression of neoplastic diseases (review). *Anticancer Res.*, **1992**, *12*(1), 235-240.

[37] Allgayer, H.; Babic, R.; Grützner, K.U.; Beyer, B.C.; Tarabichi, A.; Wilhelm Schildberg, F.; Heiss, M.M. An immunohistochemical assessment of cathepsin D in gastric carcinoma: its impact on clinical prognosis. *Cancer*, **1997**, *80*, 179-187.

[38] Sinadinović, J.; Cvejić, D.; Savin, S.; Mićić, J.V.; Janćić-Zguricas, M. Enhanced acid protease activity of lysosomes from papillary thyroid carcinoma. *Cancer*, **1989**, *6*, 1179-1182.

[39] Rochefort, H.; Capony, F.; Garcia, M. Cathepsin D: a protease involved in breast cancer metastasis. *Cancer Metastasis Rev.*, **1990**, *9*(4), 321-331.

[40] Rochefort, H. Cathepsin D in breast cancer: a tissue marker associated with metastasis. *Eur. J. Cancer*, **1992**, *28*, 1780-1783.

[41] Couissi, D.; Dubois, V.; Remacle, C.; Schonne. E.; Trouet, A. Western immunoblotting and enzymatic activity analysis of cathepsin D in human breast cancer cell lines of different invasive potential. Regulation by 17beta-estradiol, tamoxifen and ICI 182,780. Clin Exp Metastasis, **1997**, 15(4), 349-360.

[42] Rajah, T.T.; Dunn, S.T.; Pento, J.T. The influence of antiestrogens on pS2 and cathepsin D mRNA induction in MCF-7 breast cancer cells. *Anticancer Res.*, **1996**, *16*(2), 837-842.

[43] Barriga, J.; Coto, B.; Fernandez, B. Molecular dynamics study of optimal packing structure of OTS self-assembled monolayers on SiO2 surfaces. *Tripol. Int.*, **2007**, *40*, 960-966.